Quaternary Research 70 (2008) 398–411

Contents lists available at ScienceDirect

Quaternary Research

journal homepage: www.elsevier.com/locate/yqres

Two millennia of glacier advances from southern Iceland dated by tephrochronology

Martin P. Kirkbride [a,*], Andrew J. Dugmore [b]

[a] Department of Geography, University of Dundee, Dundee DD1 4HN, Scotland, UK
[b] Institute of Geography, School of Geosciences, University of Edinburgh, Drummond Street, Edinburgh EH8 9XP, Scotland, UK

ARTICLE INFO

Article history:
Received 16 November 2007
Available online 18 September 2008

Keywords:
Iceland
Tephrochronology
Moraines
Holocene
Little ice age
Medieval warm period
Dating methods

ABSTRACT

Two glaciers at Eyjafjallajökull, south Iceland, provide a record of multiple episodes of glacier advance since the Sub-Atlantic period, ca. 2000 yr ago. A combination of tephrochronology and lichenometry was applied to date ice-marginal moraines, tills and meltwater deposits. Two glacier advances occurred before the 3rd century AD, others in the 9th and 12th centuries bracketing the Medieval Warm Period, and five groups of advances occurred between AD 1700 and 1930, within the Little Ice Age. The advances of Eyjafjallajökull before the Norse settlement (ca. AD 870) were synchronous with other glacier advances identified in Iceland. In contrast, medieval glacier advances between the 9th and 13th centuries are firmly identified for the first time in Iceland. This challenges the view of a prolonged Medieval Warm Period and supports fragmentary historical data that indicate significant medieval episodes of cooler and wetter conditions in Iceland. An extended and more detailed glacier chronology of the mid- and late Little Ice Age is established, which demonstrates that some small outlet glaciers achieved their Little Ice Age maxima around AD 1700. While Little Ice Age advances across Iceland appear to synchronous, the timing of the maximum differs between glacier type and region.

© 2008 University of Washington. All right reserved.

Introduction

Iceland is the only land mass in the North Atlantic Ocean at the latitude of subpolar convergence, and it is unusual in providing records of terrestrial land-system response to changes in ocean–atmosphere circulation in a mid-oceanic setting. A comprehensive Holocene glacial history of Iceland would provide evidence of the variability in atmospheric circulation in this key region (Lamb, 1979; Guðmundsson, 1997; Stötter et al., 1999). Moraine-based chronologies lack the completeness and temporal resolution of ice cores and marine sediment proxy series, but they do provide place-specific information about cryospheric responses and allow the specific impact of ocean–atmosphere circulation changes to be measured.

This paper presents tephrochronological evidence of glacier fluctuations over a period of ca. 2000 yr, covering the Medieval Warm Period (MWP), the Little Ice Age (LIA), and the climatic transition to the warmth of the 20th century (Kirkbride, 2002). We aim (1) to reconstruct the advances of the glaciers Gígjökull and Steinsholtsjökull, to improve the quality of the Icelandic record for regional correlation, and (2) to adapt tephrochronological dating for land systems of complex origin and stratigraphy. The glaciers considered here are northern outlets from the mountain icecap Eyjafjallajökull, located in central southern Iceland (Fig. 1). The glaciers are steep, with mean gradients of 22° and 13°, respectively, and are consequently fast-responding and have no surging history. Historical activity of the Eyjafjall volcano has been limited to a possible small eruption in AD 1612, and most recently to a series of minor eruptions in the central crater (the accumulation basin of Gígjökull) in AD 1821 to 1823. Volcanism is unlikely to have influenced glacier fluctuations at other times.

Ice-marginal geomorphology

Initial geomorphological mapping was based on 1:50,000 scale topographic maps and stereoscopic aerial photographs (Icelandic Geodetic Survey 1946, 1960, 1978, 1980, and 1989). Subsequent field work integrated tephra stratigraphy from sites between moraines and on associated outwash deposits. Because moraine ridges are not contiguous around the glacier margins, sectors are defined and a separate moraine nomenclature applied to each. At Gígjökull (Fig. 2), western, northern and eastern sectors have been coded from W1 (the youngest moraine) to W9 (the oldest), N1 to N9, and E1 to E6, respectively, with no correlation between sectors implied by the numbers. Meltwater spillways are numbered S1 to S13. At Steinsholtsjökull (Fig. 3), moraines in western and eastern sectors are coded SW1 to SW5 and SE1 to SE6.

The Gígjökull moraine comprises a large arcuate ridge up to 70 m high, open to the north around the outlet from the ice-contact lake (Fig. 2). The complex morphology indicates multiple phases of deposition.

* Corresponding author.
E-mail address: m.p.kirkbride@dundee.ac.uk (M.P. Kirkbride).

0033-5894/$ – see front matter © 2008 University of Washington. All right reserved.
doi:10.1016/j.yqres.2008.07.001

https://doi.org/10.1016/j.yqres.2008.07.001 Published online by Cambridge University Press

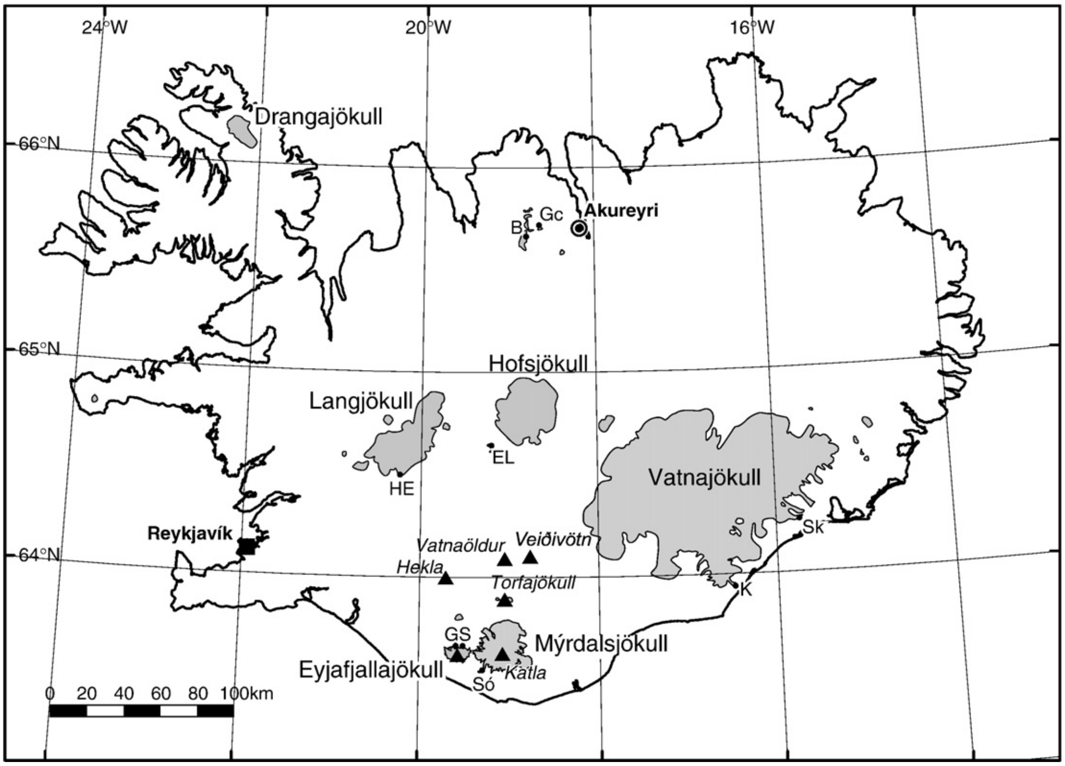

Figure 1. Iceland showing the major icecaps and the cities of Reykjavík and Akureyri. Volcanoes that have produced tephra present in the study area are shown by triangular symbols; Eyjafjallajökull is the name of both the volcano and the overlying icecap. This paper focuses on the proglacial areas of Steinsholtsjökull (S) and Gígjökull (G). Other Holocene glacial chronologies (see Fig. 11) include: Sólheimajökull (Só), Kvíárjökull (K), Skálafellsjökull (Sk), Barkárdalur and Gljufurarjokull, Trollaskagi (B, Gc), Kerlingarfjöll (EL), and Hagafellsjökull (HE).

Distal slopes are gullied by abandoned meltwater spillways that have breached the moraine crest, most of which have till "plugs" at their heads that postdate the last phase of spillway activity. All channels lead downslope into sediment fans, which allow the spatial distribution of moraines to be related to the tephra-based stratigraphy of distal glaciofluvial and aeolian deposits. Distal to moraine N7 lies a distinctive kettled fan surface associated with an outburst flood. In the eastern sector (Fig. 2), fragments of relatively old moraines protrude obliquely from the northeastern corner of the main moraine (E5 and E6). Upslope of these moraines, younger superposed moraines (E1 to E3) lie parallel to the main moraine complex. Moraine E3 is separated from the adjacent ridge by an elongate depression, infilled by sediment washed from moraines above (E1 and E2), the site of soil profile 41. Moraine E3 curves northeastwards and bifurcates (E4), indicating that ice has occupied a breach in the main rampart on at least two occasions. The breach is the site of spillway S9.

Steinsholtsjökull is confined to the narrow valley of Steinsholtsdalur (Fig. 3), containing the present ice-contact lake and, downstream, extensive kettled deposits of a large rock avalanche/debris flow in 1967 (the *Steinsholtshlaup*; Kjartansson, 1967). Four terminal moraines visible on the 1946 aerial photographs were overrun by the avalanche. Their lateral continuations are preserved on the broad ridge of Suðurhliður, where boulder ridges up to 5 m high were deposited by a lateral lobe of the glacier (SW1 to SW5 and SE1 to SE6).

Establishing an absolute chronology

Tephrochronology

Volcanoes have deposited isochronous tephra layers across the study area. Rapid aeolian sedimentation means that tephra layers are clearly separated by intervening layers of orange-brown sandy silt (Fig. 4). Individual tephras exhibit a range of macroscopic features reflecting differences in geochemistry, eruption mechanism, total tephra volume and principal directions of fallout; details are given elsewhere (Thórarinsson, 1944, 1967, 1980; Larsen, 1981, 1982, 1984, 2000; Larsen et al., 1999; Dugmore, 1987, 1989, Dugmore et al., 2000).

The geochemical fingerprints of key marker tephras have been determined by electron probe microanalysis (EPMA). Tephras were analyzed with a Cameca SX100 electron microprobe using a standard WDS (wavelength dispersive) technique, an accelerating voltage of 20 kV, a regulated beam current of 4 nA, and a rastered beam diameter of about 5μm. Ten major elements were analyzed using five spectrometers and a peak counting time of 10 s for each element. Standards of known composition, comprising a mixture of pure metals and simple silica compounds, were used for calibration. Counter dead time, fluorescence and atomic number effects were corrected using a PAP correction program. At regular periods throughout all analytical sessions, an andradite of known composition was analyzed in order to guard against unexpected variation in machine operating conditions. Original analyses (Fig. 5) confirm the provenance of tephras used as isochrons in this study.

Tephras from eruptions of the Katla, Eldgja, Hekla, Eyjafjallajökull, Torfajökull and Veiðivötn volcanoes occur in the study area (Figs. 6 to 8). Stratigraphic sections have been measured at >200 sites around Eyjafjallajökull and are supported by EPMA and radiocarbon dating (Dugmore, 1987; Dugmore and Buckland, 1991; Dugmore et al., 1992, 1995; Larsen et al., 1999, 2001). On the forelands of Gígjökull and Steinsholtsjökull, soil profiles were logged to a precision of ±2 mm. When working with truncated and disturbed soil profiles in glacier forelands, it is important also to log deep undisturbed profiles that include all the tephras to have been deposited around the study site. Four profiles measured outside the maximum extent of Holocene glaciers have been used to provide such reference profiles. These include profiles 7 and 56 in Figure 6.

https://doi.org/10.1016/j.yqres.2008.07.001 Published online by Cambridge University Press

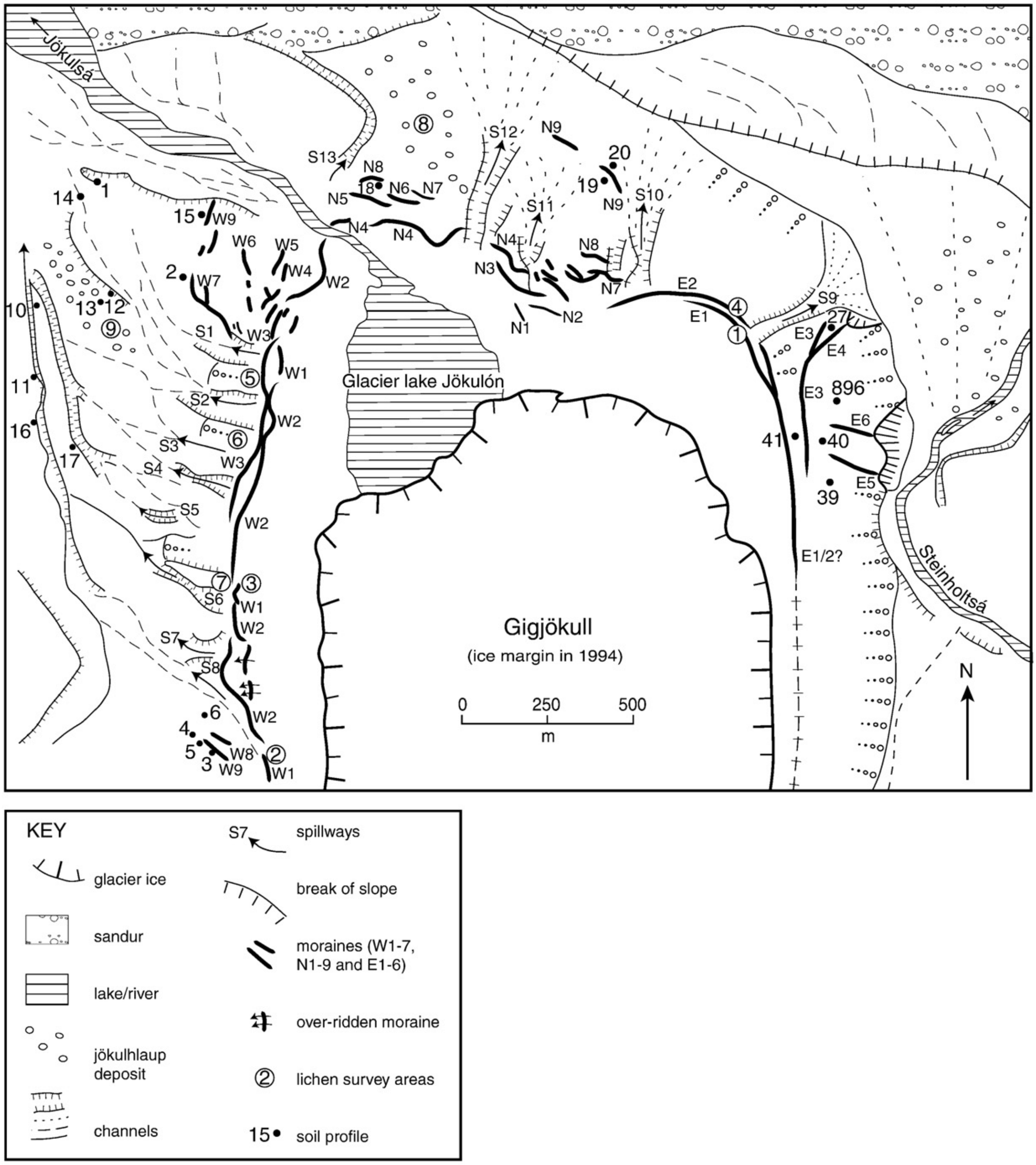

Figure 2. The geomorphology of the proglacial area of Gígjökull, with individual moraines, spillways, lichen survey sites and soil pits labeled (see text).

Field relations between tephra layers and landform age

An isochron defined by the base of a tephra layer can be used to date the contemporary land surface when the timing of an eruption is recorded in historical sources (e.g., Thórarinsson, 1967), or when the tephra's age is known from radiocarbon dating of adjacent organic material (e.g., Dugmore et al., 2000) or from ice cores (Grönvold et al., 1995). However, field relations between landforms and tephra in aeolian soils require careful interpretation, particularly where land systems contain complex stratigraphies that reflect the interplay of different process domains whose influences have changed over time; the significance of the isochron for the geomorphic history is not always readily apparent.

Figure 9 summarizes six field relations encountered in the study area. Where soil drapes over a moraine, the basal tephra in the soil profile gives the minimum age of the glacier advance (Case 1). Profiles distal to the moraine do not provide meaningful bracketing ages if they are undisturbed by moraine construction. In exposed locations, wind scour may keep the moraine crest clear of aeolian sediment. A glacier advance across a soil- and tephra-covered forefield will usually erode the soil up to the terminal moraine. In profiles distal to the moraine, the tephra subjacent to the oldest tephra found proximal to the moraine constrains the maximum age of the advance. The first tephra above the recessional till provides the minimum age in proximal profiles. Where fallout covered a partly vegetated moraine surface soon after glacier retreat (e.g., the K1721 and K1755 tephras), tephra is preserved only in the lee of boulders where tussocks prevented reworking. The K1721 tephra also occurs in interstices between boulders that are draped by younger sediment. Case 2 shows

https://doi.org/10.1016/j.yqres.2008.07.001 Published online by Cambridge University Press

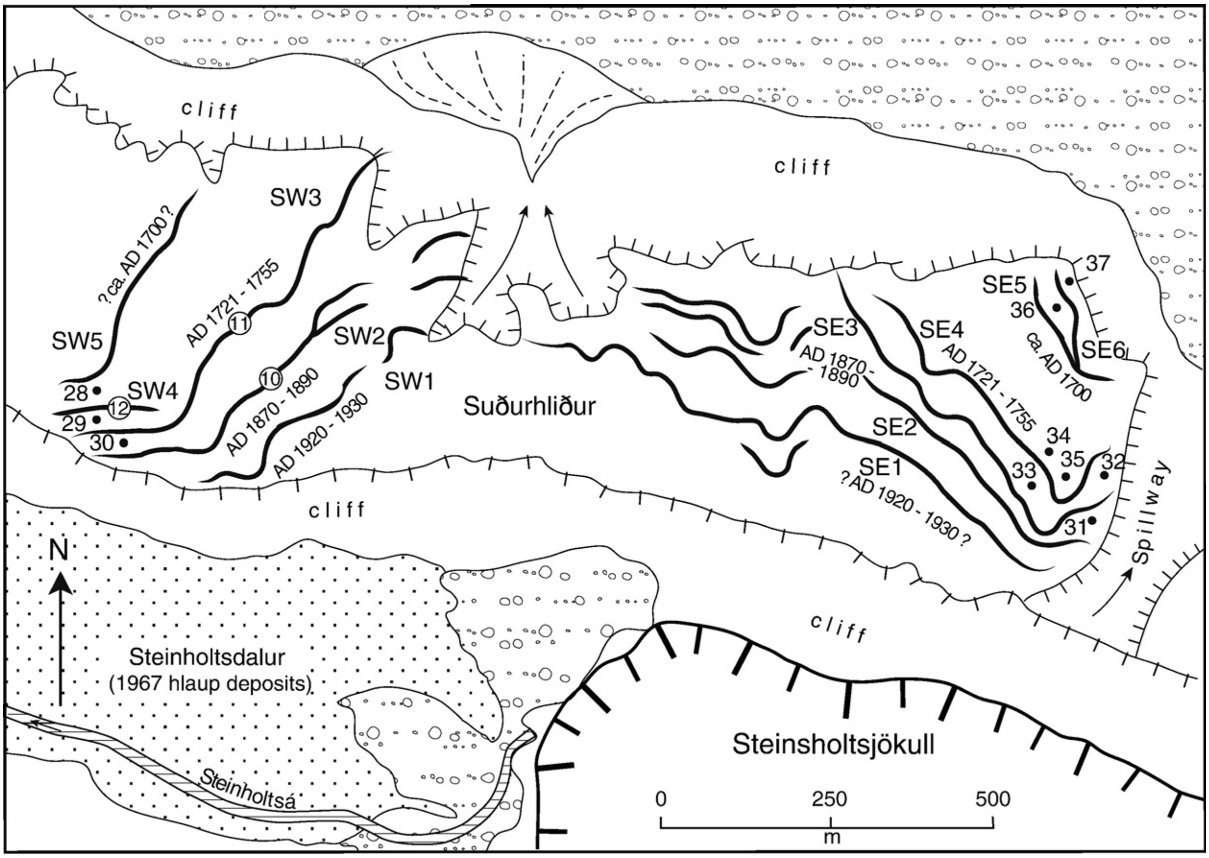

Figure 3. The geomorphology of the Suðurhliður interfluve at Steinsholtsjökull, with individual moraines, spillways, lichen survey sites and soil pits labeled (see text). Also shown are the dates derived from tephrochronology and lichenometry (Tables 1 and 2).

aeolian soil in the trough formed by a moraine built against a slope. Although the soil lies distal to the moraine, it is draped against the moraine so that the lowermost tephra again provides the minimum age of the moraine.

Interpretation is more complex when dealing with parallel moraines that channel meltwater along the inter-moraine furrows (Case 3). The basal tephra in each profile may provide minimum or maximum ages, depending on whether the location of the soil profile was scoured by meltwater during deposition of the proximal (younger) moraine. Finally, distal outwash fans contain age-significant tephras in aeolian soils both above and beneath meltwater-laid sands and gravels, in both overbank and channel-fill locations (Case 4). In overbank sediments, tephra layers sub- and superjacent to meltwater sediments provide maximum and minimum ages of meltwater activity. Below erosional contacts (e.g., close to spillway channels), the subjacent tephra may not provide a close age bracket, but this may be estimated from the youngest tephra *not* present in the sequence (which represents the last tephra to be deposited *before* the flood occurred). In channel fills, the basal tephra in the aeolian infill provides the minimum age of occupancy of the channel by meltwater. No tephra layers have been found *in situ* beneath till at Gígjökull and Steinsholtsjökull, but some profiles contain outwash intercalated with *in situ* tephra so that both maximum and minimum bracketing ages of the related glacial advance may be inferred.

Although most tephra layers occur wherever contemporary aeolian deposition predominated, some occur patchily, even in apparently continuously aggrading sequences. Patchy occurrence suggests either contemporaneous or post-depositional reworking. E1821-3, K1660, and H1597 are all represented by thin, discontinuous layers whose distribution probably reflects deposition onto snow or an unevenly vegetated surface. While their presence in a soil profile is a clear indication of age, their absence as a basal tephra is not.

Lichenometry

Long axes of thalli of *Rhizocarpon* section *rhizocarpon* lichens were measured on younger moraines and related deposits around the margins of Steinsholtsjökull and Gígjökull to improve the resolution of post AD 1821 events. Fourteen samples of between 233 and 832 thalli were collected, and data were analysed according the size-frequency method of Bradwell (2004). For each sample, the logarithms of the percentage frequency of measurements in 3-mm classes are plotted against each class mid-point. The gradient of the linear regression line fitted to classes including and larger than the modal class summarises the thallus size-structure within the sample. This can be used as a relative age indicator (e.g., Casely and Dugmore, 2004) or converted to a calendar age using a local growth curve (Bradwell, 2001). Earlier work using linear-growth rates and samples of the largest or largest five lichens on a moraine (Maizels and Dugmore, 1985; Evans et al., 1999) has been found to underestimate deposit age in the older part of the age range (Kirkbride and Dugmore, 2001a).

Bradwells' growth curve was based on calibration points in SE Iceland, a region of broadly similar near-coastal climate to the present study site. To investigate whether the curve can be applied without modification, we have plotted onto Bradwell's growth curve the size–frequency gradients of samples from the independently-dated AD 1821 *hlaup* deposit at Gígjökull and from the AD 1967 *Steinholtshlaup*.

https://doi.org/10.1016/j.yqres.2008.07.001 Published online by Cambridge University Press

A

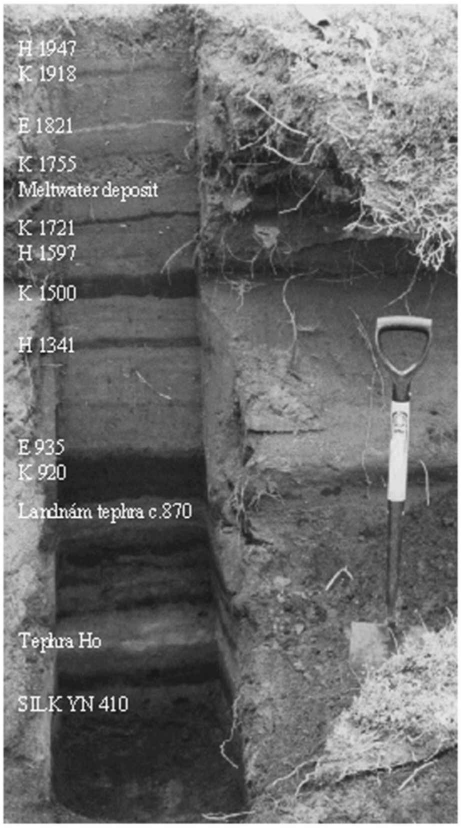

B

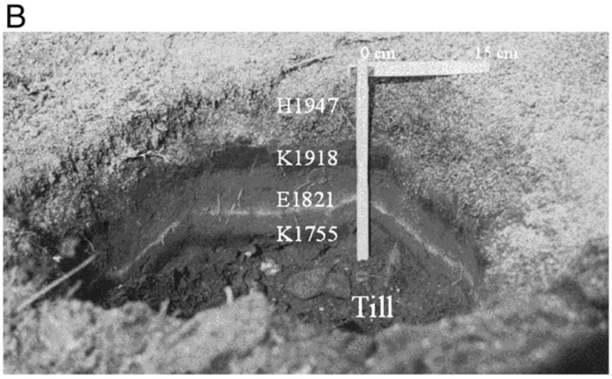

Figure 4. (A) Profile 7, an example of a complete reference section covering the last 1400 yr (Fig. 6). Tephra layers are separated by brown aeolian silt. Key marker layers are labeled. (B) Profile 19, (see Fig. 2 for location and Fig. 7 for stratigraphy), showing K1755 tephra draped over lee-side soil hummocks on moraine N9. The layers of E1821, K1918 and H1947 are visible in the overlying soil.

The former is precisely dated by association with the E1821 tephra, and the latter by direct observation (Kjartansson, 1967). Both points plot very close to the SE Iceland growth curve (Fig. 10), which is therefore adopted here. Lichenometric statistics and age assignments for each sample are presented in Table 1.

Synthesis of dated glacier fluctuations

Moraine evidence

Moraine dates fall into three distinct groups: the LIA (ca. AD 1690 to 1930); the Medieval period (8th to 12th centuries AD); and the mid-Neoglacial (Sub-Atlantic) period (ca. 2000 to 2500 ^{14}C yr BP). Tephras bounding these periods are: H1947 and H1597 (LIA); H1341 and V870 (Medieval period); and layers SILK YN (1676±12 ^{14}C yr BP) and SILK UN (2660±50 ^{14}C yr BP).

LIA moraines record multiple advances, of which four are represented at both glaciers (Table 2). Early 20th-century advances of Gígjökull, and of Steinsholtsjökull are dated lichenometrically to AD 1915 to 1936 (Table 1). A photograph of the glacier from AD 1928 shows the ice close to, but slightly below, the moraine crest, consistent with lichenometric dating. In the eastern sector of Gígjökull, moraine E1 partially overrides the 19th-century moraine E2. At Steinsholtsjökull (Fig. 3), SW1 is assigned an early 20th-century date due to the absence of the K1918 tephra within the area bounded by the moraine, and contiguity to SE1 shows this advance to have formed the proximal moraine in both sectors.

Preservation of 19th-century moraines is also good at both glaciers. At Gígjökull, lichenometric dating of E2 gives a date of AD 1847 (Table 1). The equivalent lateral moraine in the western sector (W2) is assigned the same age. At Steinsholtsjökull, moraine SW2 is dated lichenometrically to AD 1861, and the assigned age is consistent with bracketing tephra isochrons in adjacent inter-moraine furrows (Kirkbride and Dugmore, 2001a). The eastern continuation of this moraine is SE2. The age of the adjacent moraine (SE3) is bracketed by the presence of the K1918 tephra, indicating a second mid 19th-century advance at this glacier that is not found at Gígjökull. The only evidence for earlier 19th-century advances occurs at Gígjökull, where moraine N7 grades into a kettled outwash fan that predates the K1918 tephra and is probably associated with the local eruption and outburst flood associated with the E1821 tephra (see below).

Advances in the mid-18th century are widespread and closely bracketed by the K1721 and K1755 tephras. One advance of Gígjökull deposited moraine fragments W8 and N9 shortly prior to the K1755 tephra fall, and after the K1721 eruption (profiles 19 and 20; Fig. 4b). Soil cover bounded by the moraine surface and the K1755 isochron was thin and patchy, in places forming tussocks in the lee of morainic boulders. The advance probably predated the tephra fall by only a few years. At Steinsholtsjökull, two moraines (SW3 and SW4) are bracketed by these tephras, of which one possible correlative (SE4) occurs to the east. Lichenometric dating of moraines SW3 and SW4 give anomalous mid-19th century dates (Table 1), but the tephra isochrons are unequivocal in demonstrating a mid-18th century age.

Such cross-dating indicates that lichenometry alone gives a false impression that 19th-century advances represent the LIA glacial maximum. The lichenometric method employed here contrasts with the earlier linear-growth approach applied to the same samples by Kirkbride and Dugmore (2001a). A linear-growth curve produced moraine dates several decades younger than those presented here, but neither method is consistent with the tephrochronological results.

Glacier advances from ca. AD 1700 are represented by Gígjökull moraine W9 (profile 15, Fig. 2) and Steinsholtsjökull moraines SE5, SE6 and possibly the undated SW5 (Fig. 3). All predate the K1721 tephra, but no close maximum age is available because the next oldest tephra in the regional sequence is the patchy H1597 layer (reference profile 7, Fig. 6). The K1721 tephra occurs as a discontinuous layer on these moraines at sites where a continuous soil and vegetation cover had developed before the K1755 ash draped over the moraine surface. By implication, the lack of soil accumulation between moraine deposition and the AD 1721 eruption places the advance probably within two decades of the tephra fall, and a date of ca. AD 1700 is assigned. The earlier of the two advances close to this time represents the earliest dated LIA activity at the two glaciers.

The next oldest surviving glacial deposits are separated by an interval of at least 360 yr. Medieval advances are represented by

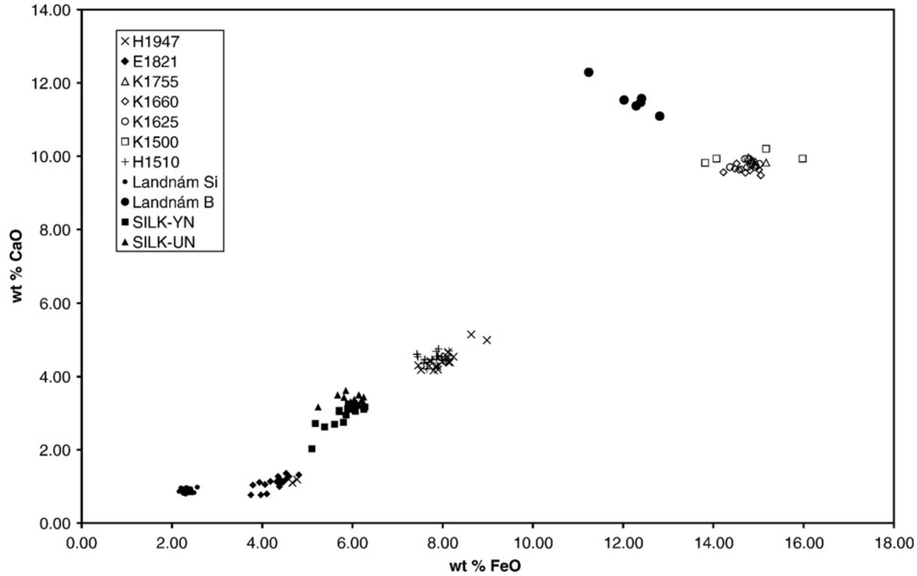

Figure 5. Comparison of the geochemistry of selected tephra layers in the study area with reference analyses (Larsen et al., 1999, 2001). Each symbol represents the analysis of an individual grain of glass. Both the silicic and basic components of the Landnám tephra layer are present. Other tephra compositions range from the highly silicic (>70% SiO_2) E1821 tephra, through intermediate compositions of both Hekla (e.g., H1510) and Katla tephras (e.g., SILK YN) to the basic Katla tephras (e.g., K1755). Complete results are recorded in an ORACLE database held at the Department of Geography in the University of Edinburgh (www.geo.ed.ac.uk/tephrabase).

moraines E3 and E4 at Gígjökull. The age of E3 is constrained by the H1341 tephra but the absence of E935 in profile 41 (Fig. 7). Extrapolated soil accumulation suggests a date between ca. AD 1035 and 1165, but historical records suggest that glacier expansion may have resulted from severe winters between AD 1181 and 1187, 1193, 1197 to 1200, and 1203 to 1204 (Ogilvie, 1984). Moraine E4 is older, and its maximum age is constrained by the V870 tephra and three older prehistoric tephras between the two moraines (profile 27, Figs. 2 and 7). Extrapolation of soil accumulation places the date of glacier advance at ca. AD 700.

Two middle Neoglacial advances are represented by moraines E5 and E6 at Gígjökull. Tephra SILK YN (1676±12 ^{14}C yr BP, AD 338 to 418; Dugmore et al., 2000) occurs inside E5 and E6 (profiles 39 and 40), providing the minimum age for both moraines. The maximum age is indicated by the *absence* of the SILK UN tephra (2660±50 ^{14}C yr BP, 917 to 777 BC) in aeolian soil proximal to the moraines. This tephra occurs as a >5-mm layer in soils close to the Gígjökull moraine complex (Larsen et al., 2001). It is absent from truncated profiles within the glacier foreland when the underlying sediment postdates the tephra fall. Over a period of at least eight centuries, the Greenland δ^{18}O record (Fig. 11) suggests a climate favourable for glacier expansion only in the 3rd century AD. These moraines are correlated with the Barkárdalur I stage (ca. 1835–2240 cal yr BP) in Tröllaskagi and the Ystagil stage at Sólheimajökull (Kirkbride and Dugmore, 2001b).

The western spurs of the Gígjökull moraine complex appear to be the eroded remnants of pre-LIA moraines but cannot be dated. The lichen ages of samples 5 to 7 (Table 1) are beyond the calibration range for the technique.

Spillway evidence

Most soil profiles in which sediments record meltwater activity were excavated in the banks of relict channels. Soil sequences comprise aeolian silt, tephra, sand and gravel, occasionally overlying eroded contacts. Sand and gravel layers represent sheet-flow and overbank sedimentation, recording periods of high meltwater discharges in adjacent spillway channels and across fan surfaces, and therefore periods when the glacier overtopped the moraine crest. Channel lag deposits are recorded only in the locality of exceptional events, notably the AD 1821 *hlaup* deposit (Figs. 2 and 6: profiles 12, 13A and 13B).

Table 3 shows periods for which the stratigraphy records spillway activity in the western sector. Most recent activity occurred in the 19th century, as shown by outwash gravel underlying the K1918 tephra. Outwash sediments overlie eroded contacts in several localities, removing evidence of earlier activity. For example, 19th century meltwater in profile 10A has removed earlier LIA tephra layers down to H1597. Evidence of early LIA meltwater activity (between the H1597 and K1721 tephras) survives in profiles 11 and 16 (Fig. 6), indicating the glacier discharging meltwater into spillways S6 to S8 shortly before AD 1721. An advance at that time is recorded by moraine W9, correlating with Steinsholtsjökull moraines SE5 and SE6. More precise dating using extrapolated sediment accumulation rates is not possible due to unconformities within the soil profiles.

The base of soil profiles in the western sector is a coarse gravel or boulder lag. The lowest tephras in individual profiles are variously V870, KR 920, E935 or H1341, indicating that the basal lag is diachronous (Fig. 6). Its formation shortly prior to these tephras possibly records widespread meltwater erosion between the 9th and 13th centuries, predating the LIA by several centuries.

The northern spillways (S9 to S13) are dated by the ages of their associated moraines and therefore record only the last period of activity (Table 3). S9 and S13 (and possibly S10) were active during early 20th-century advances that discharged meltwater through the northern breach in the main moraine. These spillways truncate earlier moraines and outwash features (N9, E2, and the AD 1821 fan). The present stream is the only outflow still active.

Spillway evidence in the western sector demonstrates that the moraine complex has a longer constructional history than is revealed by dating the superficial mantle of LIA moraine ridges, and that Gígjökull's outflow has become concentrated in the northern sector as the lateral moraine crest has been raised. Superposition of multiple tills since before the MWP means that visible moraine ridges represent only the youngest of a history of

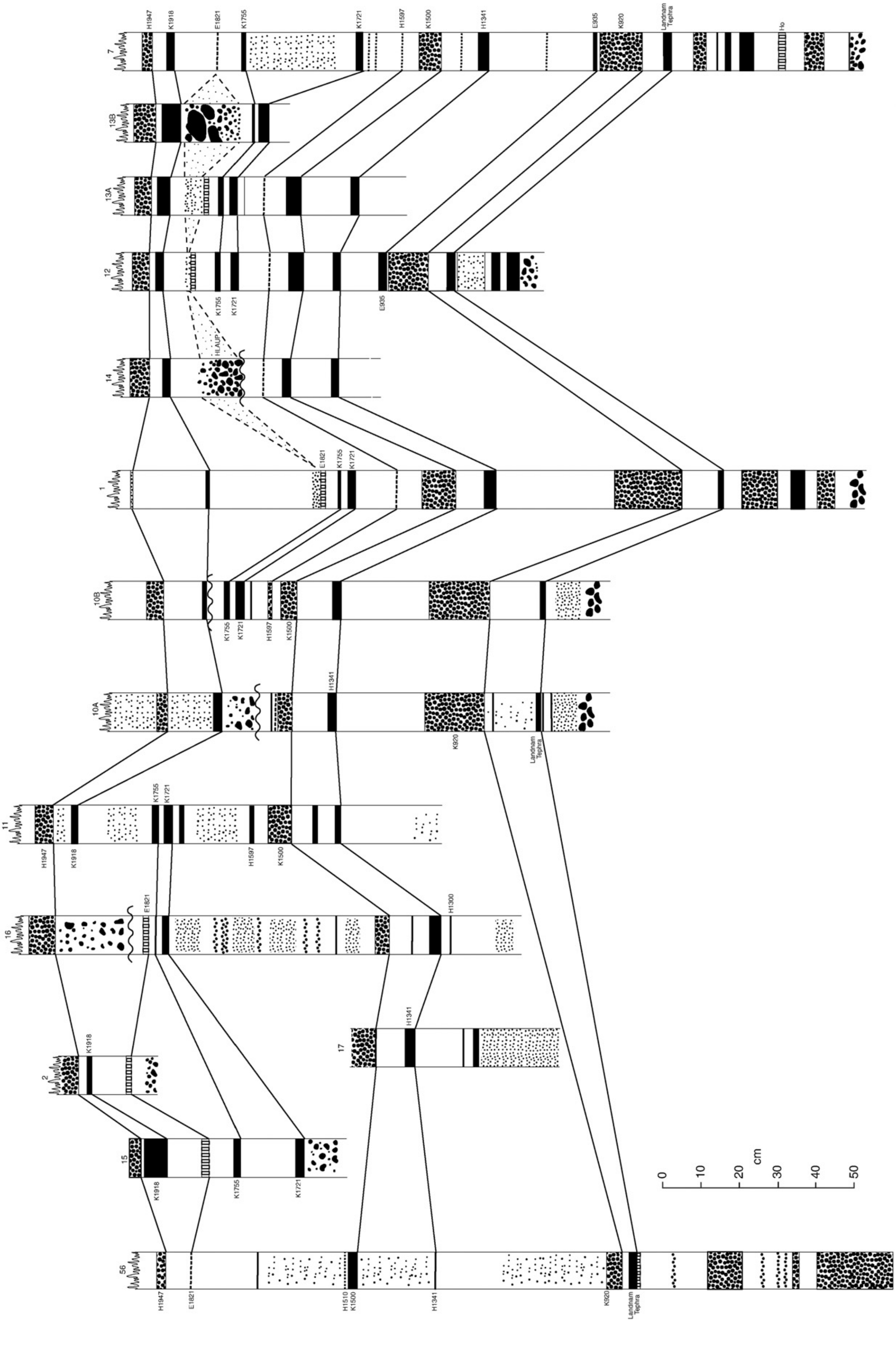

Figure 6. Stratigraphic columns for the proglacial areas of west of Gígjökull. For locations see Fig. 2. Abbreviations used for the source volcanoes of identified tephra layers: H, Hekla; K, Katla; SILK, Katla (silicic tephra); E1821, Eyjafjallajökull; E935, Eldgjá; Landnám tephra, Vatnaöldur/Torfajökull.

https://doi.org/10.1016/j.yqres.2008.07.001 Published online by Cambridge University Press

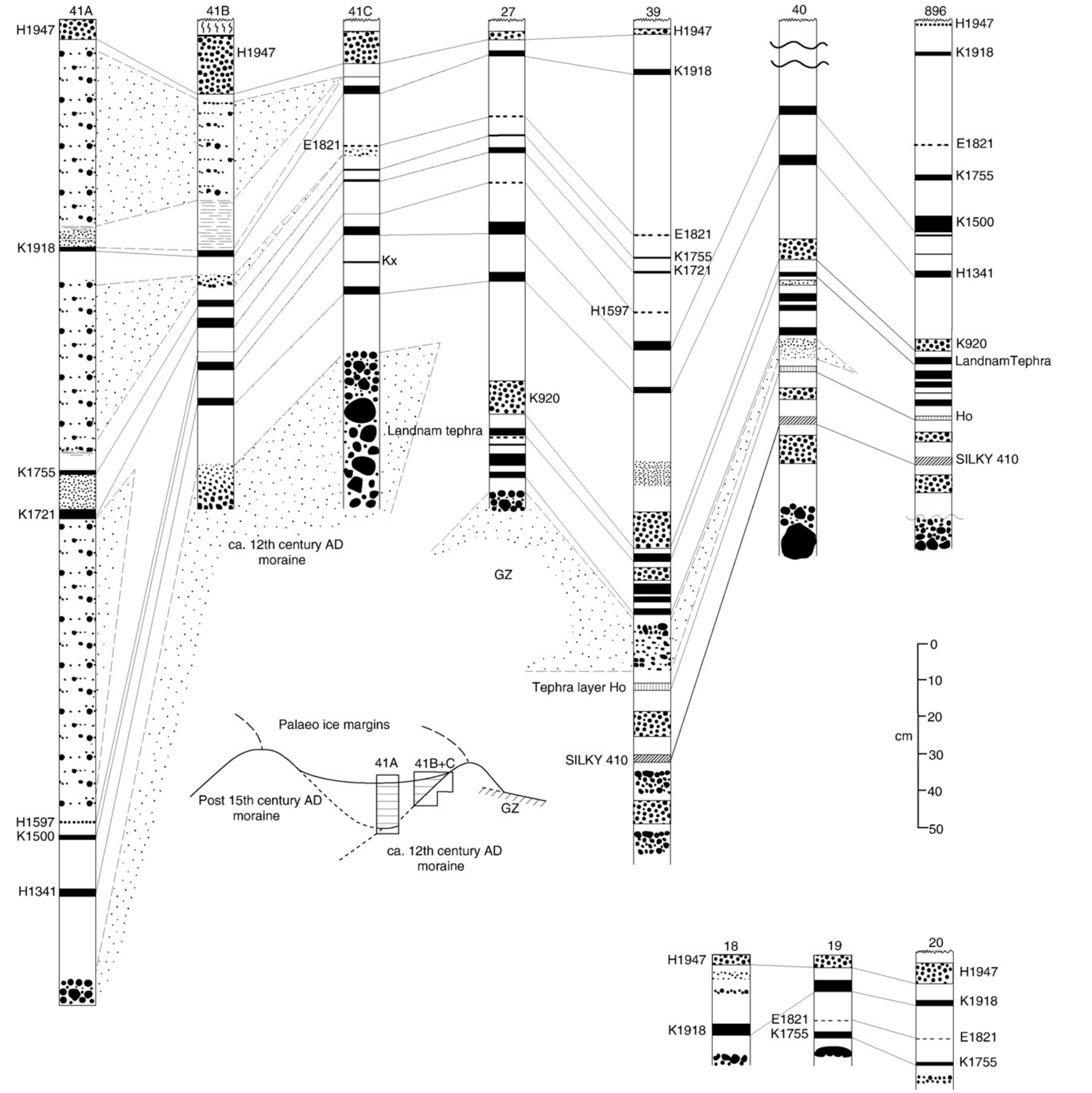

Figure 7. Stratigraphic columns for the proglacial areas north and east of Gígjökull. For locations see Fig. 2. Abbreviations used for the source volcanoes of identified tephra layers: H, Hekla; K, Katla; SILK, Katla (silicic tephra); E1821, Eyjafjallajökull; E935, Eldgjá; Landnám tephra, Vatnaöldur/Torfajökull.

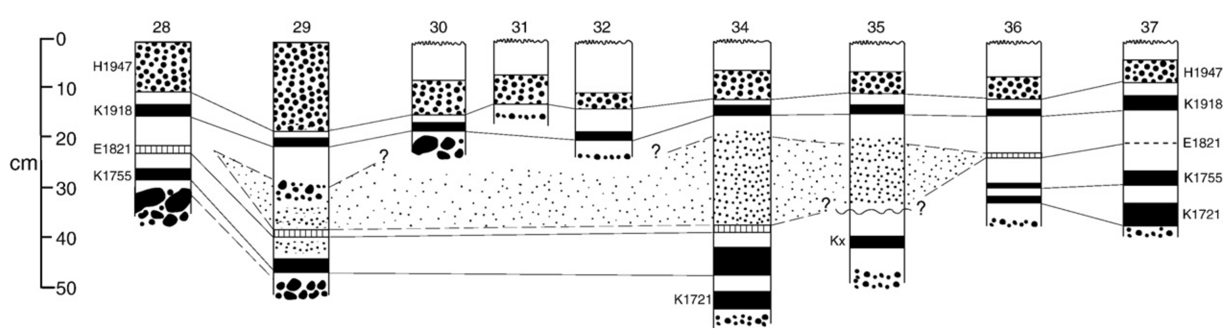

Figure 8. Stratigraphic columns for the proglacial area north of Steinholtsjökull. For locations see Fig. 3. Abbreviations used for the source volcanoes of identified tephra layers: H, Hekla; K, Katla; SILK, Katla (silicic tephra); E1821, Eyjafjallajökull; E935, Eldgjá; Landnám tephra, Vatnaöldur/Torfajökull.

https://doi.org/10.1016/j.yqres.2008.07.001 Published online by Cambridge University Press

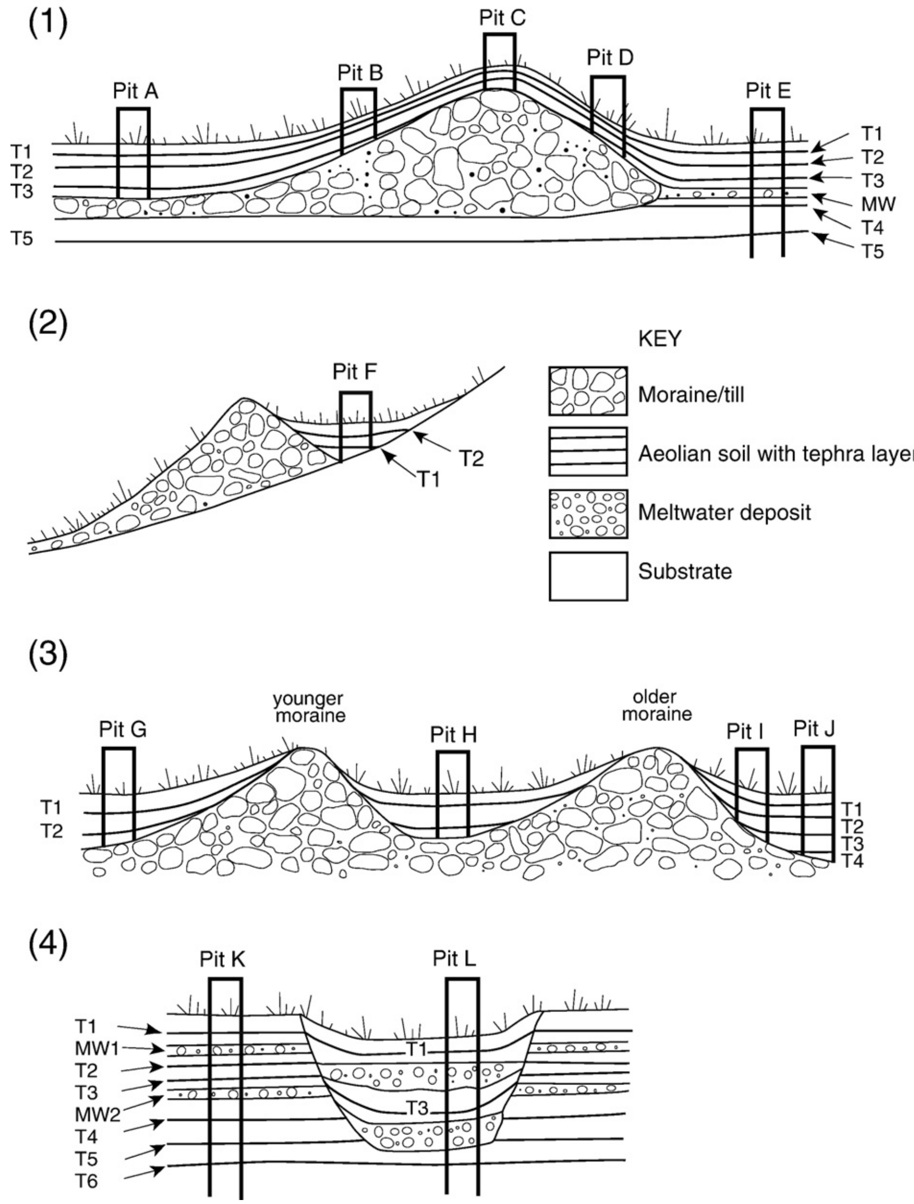

Figure 9. Schematic explanation of field relations: (Case 1) Stratigraphy depends on location of profile on a moraine draped by aeolian soil and tephra layers T1 to T5. Note the thinning and pinching out of the soil layer over the moraine crest. Pits A, B and D provide the closest minimum age for the moraine. Pit E provides maximum (T4) and minimum (T3) ages for the advance if the meltwater layer (mw) can be related to the moraine. (Case 2) Trapping of sediment in a distal furrow provides a minimum bracketing age (T1). (Case 3) Pit G provides a minimum age for the younger moraine (T2). The same stratigraphy distal to the moraine (Pit H) indicates meltwater scouring of the inter-moraine furrow from the younger moraine. Therefore, Pit H also provides a minimum age for this moraine, but cannot be used to date the older moraine, whose minimum age is given by Pit I. Pit J cannot be used because the sediment here may predate the earlier advance. (Case 4) Example of an outwash fan section. Pit K provides close maximum and minimum ages for two overbank meltwater events (mw1, mw2). Pit L in an infilled spillway provides close minimum ages for both events (T1 and T3) but erosional lower contacts of each meltwater layer preclude close maximum bracketing ages.

advances whose existence can only be inferred from glacial meltwater deposits buried within aggrading fans, and which have few (if any) preserved moraine remnants.

Landforms related to the Eyjafjalljökull AD 1821 eruption and outburst flood

A small explosive eruption in AD 1821 to 1823 in the central crater of Eyjafjalljökull deposited tephra within 10 km of the volcano (Larsen et al., 1999). Two areas around Gígjökull appear to have acted as flood routeways for a *jökulhlaup* that accompanied the start of the eruption. In the western sector (Fig. 2), an outwash fan surrounding spillway 2 is strewn with unusually large boulders. Soil profiles linking the boulder deposit and the spillway with the E1821 tephra provide stratigraphic evidence for the AD 1821 *hlaup* as the formative event for the fan (Fig. 6, profiles 12 and 13: Kirkbride and Dugmore, 2001a). In the northern sector, two moraines are linked to the 1821 event. N7 merges with a kettled outwash fan, unlike other outwash surfaces around the glacier, overlain by the K1918 tephra but not the K1755 tephra. Moraine N4 contains pumice clasts from the AD 1821 to 1823 eruption within its till matrix. It appears that N7 was deposited close to the time of the initial eruption and outburst flood in AD 1821, though it may predate the eruption and have survived the outburst flood. Lichens on both *hlaup* deposits suggest mid-19th century dates, which underestimates their age by several decades, though by less than

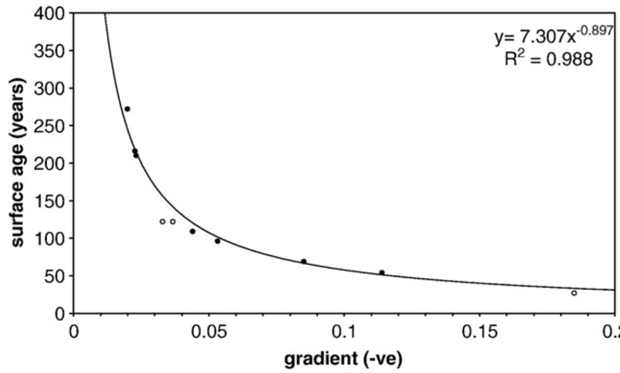

Figure 10. Calibration curve of population gradient against deposit age for *Rhizocarpon* section *rhizocarpon* lichens in southeast Iceland (Bradwell, 2001). The open circles represent samples from the Steinsholtshlaup deposit of AD 1967 and from the AD 1821 *hlaup* at Gígjökull. Both show a close correspondence to the calibration curve.

calculated by the linear-growth model (Kirkbride and Dugmore 2001a).

Discussion

Table 4 summarizes glacier advances and correlations between Gígjökull and Steinsholtsjökull. Preceding the well-documented AD 1970 to 1990 advance, LIA advances appear to have occurred in or around the following decades: AD 1880 to 1920; early AD 1800s; AD 1740; and AD 1700. These are best estimates within the constraints provided by the dating methods employed. Buried meltwater sediments at Gígjökull suggest repeated glacier highstands before AD 1700 that are not represented by moraines. Earlier advances dated to ca. AD 1180 to 1200, AD 700 to 900, and AD/BC 0 extend the known chronology of glacier fluctuations in Iceland. These advances correspond to "Little Ice Age-type events" (LIATEs) 1 to 4 and 5 or 6, using the terminology of Kirkbride and Dugmore (2006).

Discussions of synchroneity and asynchroneity in regional reconstructions of glacier advances must be qualified by the timescale under consideration, and by a careful distinction between the timing of individual advances and the timing of the maximum advance. The former may be synchronous across a region while the latter may still be asynchronous.

Synchroneity of advances

Gígjökull and Steinsholtsjökull represent well-preserved and well-dated proxies for short-term (decadal) climatic deteriorations superimposed on more prolonged (century-scale) cool periods. Correlations between glacier chronologies within Iceland, and with climatic proxy evidence, must take three issues into account. First, the moraine record rapidly becomes more incomplete the further back in time one looks. Evidence of earlier advances is tantalisingly fragmentary and more difficult to date due to erosion censoring by 18th and 19th century glacier advances and by jökulhlaups affecting some forelands. Thus, an absence of evidence does not necessarily indicate evidence of an absence of a climatic event (Casely and Dugmore, 2004). Second, evidence of climate variation becomes richer, more direct, and more quantitative towards the present (Fig. 11). Only ice core data provide a high-resolution record over two millennia, but from a distant site (O'Brien et al. 1995). Pinpointing the climatic conditions associated with periods of glacier advance therefore becomes more certain towards the present. In Figure 11, recent glacioclimatic associations have been used to inform interpretations of the timing of earlier glacier advances. Third, it is difficult to compare local glacier chronologies dated by different lichenometric techniques. Several earlier lichenometric studies predating that of Evans et al. (1999) do not provide results comparable to Bradwell's (2004) population-gradient method, and they have not been considered here.

With circumspection, it is possible to make some comment on the significance of our findings. The best-documented glacier advances, those in the 20th century AD, have been synchronous across Iceland (Sigurdsson, 1998). Many glaciers reached maxima in the early 1990s following climatic deterioration two to three decades earlier. The late 19th century advance also affected most glaciers across Iceland within a few decades. The logical inference is that earlier advance periods would also have been synchronous across the island, at least for those fast-responding glaciers whose timescale for mass adjustment was shorter than the frequency of the climatic forcing. Where evidence seems to indicate a regionally asynchronous response, it would be premature to invoke regional climatic differences without first discounting issues of preservation, dating, and system response characteristics (Kirkbride and Brazier, 1998; Kirkbride and Dugmore, 2006).

Post-AD 1700, four periods of glacier readvance can be correlated with other glaciers in Iceland and with climatic data series (Fig. 11). Each period was associated with some combination of cold winters and/or cool summers as indicated most recently by the instrumental record, and prior to this by reconstructed sea-ice and thermal index proxies (e.g., Bergthórsson, 1969; Ogilvie, 1992). Most cases of glacier advance correspond to a greater frequency of the negative winter index of the North Atlantic Oscillation (NAO) (Kirkbride, 2002; Bradwell et al., 2006); however, all four main periods of LIA readvance are associated with frequent negative summer NAO indices. Furthermore, all correspond to negative $\delta^{18}O$ anomalies in the GISP2 ice core indicating that such excursions can be used to infer the timing of poorly constrained advances earlier in the record, as suggested in Figure 11.

The significance of the maximum LIA glacier extent

Synchronous 20th-century glacier advances across Iceland imply that there should also be preserved an island-wide geomorphic record of the period most favourable to glacier expansion within the LIA. The LIA is characterised by glacier readvances of similar magnitude since ca. AD 1700, which have at least partly censored the landform record of earlier advances. A long-term increase in the

Table 1
Lichenometry statistics and age assignments

Sample site	Sample number	*n*	Size–frequency gradient	Date of substrate stabilisation	Largest lichen (mm)
Gígjökull					
Moraine W1	2	689	−0.0715	AD 1915	42
Moraine W1	3	649	−0.0866	AD 1927	40
Moraine E1	1	459	−0.1014	AD 1936	33
Moraine E2	4	839	−0.0356	AD 1847	89
AD 1821 *hlaup* northern fan	8	706	−0.0367	AD 1851	80
AD 1821 *hlaup* western fan	9	748	−0.0259	AD 1799	121
Moraine spur	5	233	−0.0240	AD 1786	76
Moraine spur	6	304	−0.0233	AD 1780	97
Moraine spur	7	233	−0.0291	AD 1819	77
Steinsholtsjökull					
Moraine SW2	10	550	−0.0398	AD 1861	69
Moraine SW3	11	718	−0.0380	AD 1856	80
Moraine SW4	12	482	−0.0316	AD 1831	81
AD 1967 *hlaup*	13	671	−0.1849	AD 1960	19

https://doi.org/10.1016/j.yqres.2008.07.001 Published online by Cambridge University Press

Table 2
Age assignments for the Gigjökull moraines

Moraine	Tephras				Lichens	Notes
	Maximum bracket	Minimum bracket	Best estimate	Soil profile & field relations (see Fig. 9)		
E1	K1918	H1947	–	Profile 41 (1:E)	1936	Partially overrides E2
E2	K1918	H1947	–	Profile 41 (1:E)	1847	Pre-dates spillway 9
E3	K920	H1341	(1) 1035 – 1164 (2) **1181 – 1204**	Profile 41 (1:A)	–	(1) By accumulation rate (2) By comparison with documentary records
E4	?	V870	**ca. 700–900**	Profile 27 (1:A)	–	First evidence of pre-MWP advance in Iceland
E5	SILK UN	SILK YN 345–419	0 AD/BC	Profiles 39, 40 (4:K)	–	"Subatlantic" period
E6	SILK UN	SILK YN 345–419	0 AD/BC	Profile 40 (1:A)	–	"Subatlantic" period
N1-3	–	H1947		(3:G)	–	1920–1930 recessional sequence
N4	–	–	–	–	–	Contiguous with W2
N7	E1821	E1821	**ca. 1821**	(1:E)	–	Tephra occurs within moraine
N8	–	–	–	Profile 18 (3:H)	–	Undated—fragment of N7?
N9	K1721	K1755	**ca. 1740s**	Profile 19 (1:A) Profile 20 (3:J)	–	
W1	–	–	–	–	1915–1927	"Plugs" spillways in W2
W2	–	–	–	–	–	Correlative of E2 by location (ca. 1874)
W7	H1597	K1721	**1700s**	Profile 15 (1:E)	–	
W8	K1721	K1755	**ca. 1740s**	Profiles 5 (3:J), 6 (3:G)	–	
W9	H1597	K1721	**ca. 1700s**	Profiles 5 (2:F), 11 (1:E), 41 (1:E)	–	Earliest preserved LIA advance
SW1	K1918	H1947	**ca. 1920s – 30s**	–	–	Dated partly by location (most proximal ridge)
SW2	E1821	K1918	–	Profile 30 (2:F)	1861	Lichenometry consistent with tephrochronology
SW3	K1721	K1755	**ca. 1740s**	Profile 29 (2:F)	1856	Lichens underestimate moraine age
SW4	K1721	K1755	**ca. 1740s**	Profile 28 (3:H)	1831	Lichens underestimate moraine age
SW5	–	–	–	–	–	Undated but older than SW4
SE1	–	–	–	–	–	Contiguous with SW1 (1920s–1930s)
SE2	–	–	–	–	–	Contiguous with SW2 (1880s)
SE3	E1821	K1918	**ca. 1880s**	Profile 32, (3:H)	–	
SE4	K1721	E1821	**ca. 1740s**	Profiles 34 (3:J), 35 (2:F)	–	Profile 34 also shows destabilisation between 1821 and 1918.
SE5	H1597	K1721	**ca. 1700s**	Profile 36 (3:J)	–	
SE6	H1597	K1721	**ca. 1700s**	Profile 37 (3:J)	–	

Figures in bold type are preferred age estimates. Ages are in yr AD.

frequency and magnitude of negative δ^{18}O anomalies in central Greenland (Fig. 11) suggest that earlier LIA advances in Iceland would have been of lesser extent. Thus, at the millennial scale, the LIA glacier maximum occurred in the later part of the post-MWP period.

At the century scale, significant regional variability is apparent and any one of several periods of readvance identified above may represent the LIA maximum. At Gígjökull and Steinsholtsjökull the LIA maximum occurred prior to AD 1721; in central Iceland (Kirkbride and Dugmore, 2006) prior to AD 1721 at some small glaciers, and prior to AD 1766 at another; elsewhere, an early 19th century maximum occurred at the western outlets of Mýrdalsjökull (Casely and Dugmore, 2004) and at several glaciers in SE Iceland (Bradwell, 2004; McKinzey et al., 2004; Bradwell et al., 2006) as well as in the Trollaskagi Peninsula in the north (Caseldine, 1991; Caseldine and Stötter, 1993; Kugelmann, 1991). An LIA maximum in the late 19th or early 20th century has been proposed for many large icecap margins and outlet glaciers (Evans et al., 1999). While some glaciers undoubtedly did reach their greatest extent in this period, recent research has shown that many peaked earlier.

Variation in the timing of the maximum extent reveals at best a weak regional pattern, and this may relate to the response characteristics of the dominant glacier type in a region. Where ice cap lobes occur in the same area as small mountain glaciers, they have later LIA maxima (Kirkbride and Dugmore, 2006). The preservation potential of deposits in different proglacial environments is also an issue (Casely and Dugmore, 2004; cf. Kirkbride and Brazier, 1998). Thus, it is doubtful whether regional climatic signals can be inferred from differences in the timing of the LIA maximum across Iceland.

The growing body of empirical data points to the absence of a single LIA maximum. If some of the differences in the timing of local glacier highstands are due to the spectrum of timescales of glacier response, this potentially provides a finely tuned set of responses for calibrating high-resolution glacier modeling aimed at understanding differing glacier response rates. It also reveals the nature of different phases of climate fluctuation: for example, the lack of island-wide correlatives of Gígjökull's advance at ca. AD 1190 to 1200 may imply that the duration of the climatic cooling was shorter than the response rate of the larger glaciers and ice caps.

A potential complication in an active volcanic region is the impact of airfall tephra on glacier ablation. Even modest tephra falls may trigger minor advances (10^1 to 10^2 m) lasting a few years. The timing of local tephra deposition may modify the detail and precise timing of glacier highstands (Kirkbride and Dugmore, 2003). The AD 1740s highstand at Gígjökull may have been aided by supraglacial tephra from the Katla eruption in AD 1721, though the general increase in ice volume in the 17th century must reflect climatic deterioration primarily, there being no significant tephra falls between AD 1597 and 1721. Elsewhere, where tephra falls occurred several times per decade (for example Grimsvotn fallout over parts of Vatnajökull) repeated episodes of tephra deposition on ablation zones may have induced a greater non-climatic mass balance response.

As more field studies employ tephrochronological dating at smaller glaciers in Iceland, a picture of later Holocene glacial history emerges that is quite different from that portrayed by lichenometric studies alone. Forelands with better landform preservation furnish longer and more detailed moraine chronologies, from which a

https://doi.org/10.1016/j.yqres.2008.07.001 Published online by Cambridge University Press

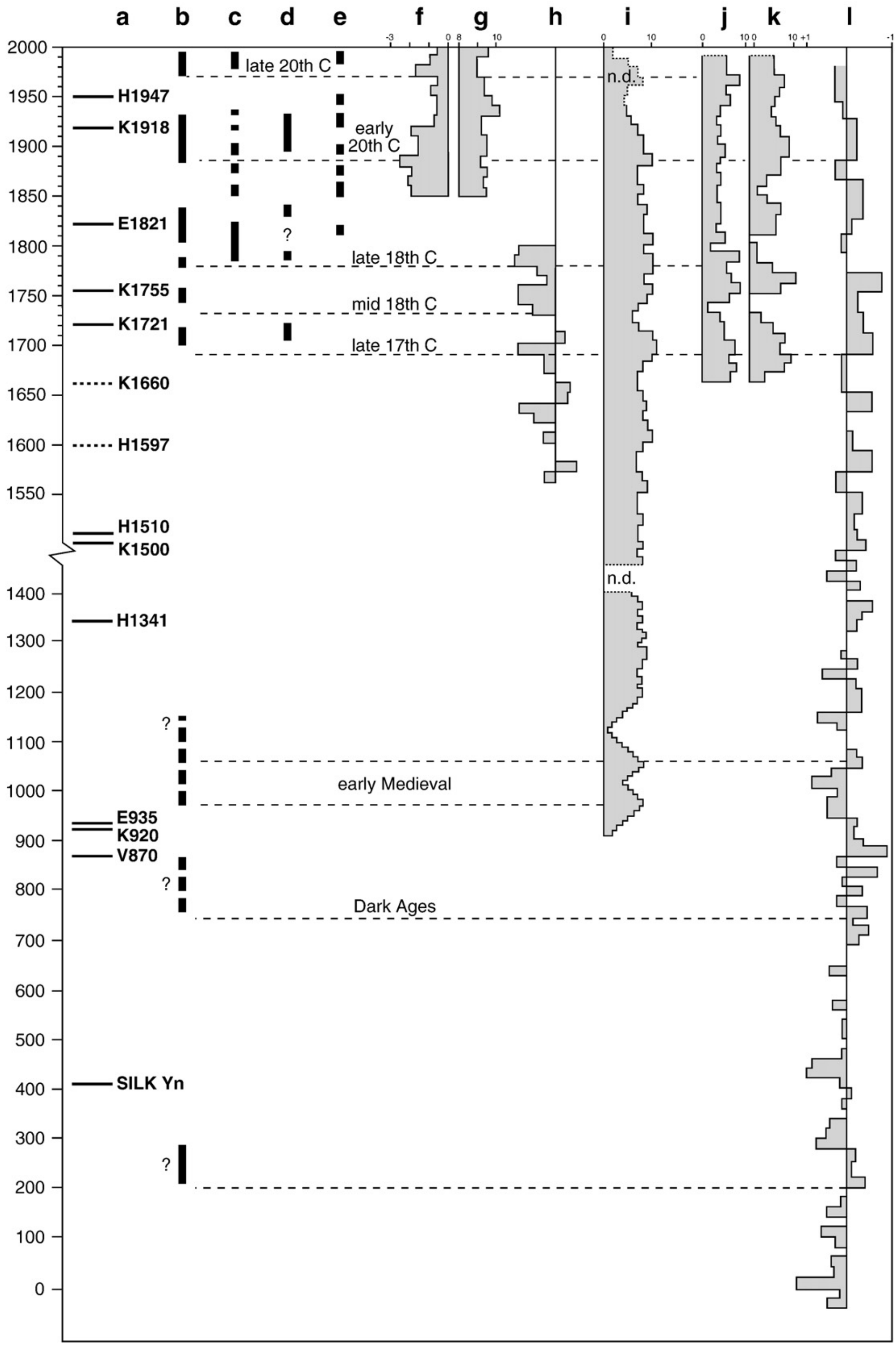

Figure 11. A synthesis of periods of moraine formation in different regions of Iceland and of climatic data at the decadal timescale over the last two millennia. Dashed horizontal lines indicate correlations between variables. Key: (a) tephra layers in the study area; (b) to (e) best estimates of the timing of moraine formation in (b) south Iceland (this study and Casely and Dugmore, 2004), (c) south-east (McKinzey et al., 2004; Bradwell et al., 2006) (d) central (Kirkbride and Dugmore, 2006) and (e) northern Iceland (Caseldine, 1985, 1991; Kugelmann, 1991); (f) mean decadal winter temperature (Dec-Feb); (g) mean decadal summer temperature (JJA), both from Stykkisholmur; (h) Ogilvie's (1992) winter-spring thermal index, based on documentary sources of severe climate throughout Iceland; (i) Bergthorssen's (1969) sea-ice index (0 = low incidence, 10 = high incidence); (j) winter (DJF) reconstructed NAO (number of negative winters per decade based on Luterbacher et al., 1999); (k) summer (JJA) NAO (number of negative summers per decade); (l) bidecadal GISP2 $\delta^{18}O$ anomalies from the mean value for the last two millennia. Fig. 1 shows locations of glacial moraines summarized by (b) to (e).

https://doi.org/10.1016/j.yqres.2008.07.001 Published online by Cambridge University Press

regionally synchronous pattern of the main periods of glacier growth is increasingly evident.

Conclusions

The earliest LIA advances so far identified in south Iceland are dated to the late 17th to early 18th century AD, with several advances preceding those of the late 19th century. The main periods of advance correlate with dated moraines elsewhere in Iceland: significant advances occurred in the AD 1700s, 1740s, the late 17th to early 18th centuries, the early and late 19th century, and the late 20th century.

The LIA appears to have been characterized by repeated phases of glacier expansions of similar magnitude that were broadly synchronous at the century timescale. Local differences in the timing of their greatest extent (the "LIA maximum") probably relate to differences in glacier response characteristics and moraine preservation rather than to a regional climatic signal.

At Gígjökull, advances occurred between the 10th and 12th centuries AD and are believed to relate to cool climate in the 1190s to 1200s. One moraine predates the V870 (Landnam) eruption and probably formed in the 9th century AD.

Two advances occurred between 1700 and 2300 cal yr BP, and correlate with the Barkárdalur I stage (ca. 1835 to 2240 cal yr BP) in Tröllaskagi and the Ystagil stage at Sólheimajökull.

These findings extend the range and detail of the record of Icelandic glacier fluctuations in the later Holocene, with implications for the interpretation of the palaeoclimatic proxy record, and they show that further potential exists for constructing well-dated glacial chronologies based on detailed tephrostratigraphic studies.

Acknowledgments

Funding for this project was provided by the Carnegie Trust for the Universities of Scotland, the Leverhulme Trust and by the Royal Society (Grant 571310.V706/LUM/TH). Field assistance by Ann Davies, Mark Skidmore, Nick Spedding, David and Michael Sugden is gratefully acknowledged. Geochemical analyses were undertaken at the Department of Geology, University of Edinburgh, with the support of Peter Hill and Anthony Newton, and Gerry White produced the diagrams. The paper benefited from the refereeing of Tom Bradwell, Chris Caseldine, Atle Nesje, and anonymous referees.

Table 3
Periods of activity of meltwater spillways at Gigjökull for which stratigraphic control is available

Spillway	Dates of past activity					Notes
	20th century	19th century	17th century	Mediaeval	Pre-Mediaeval	
Western sector						
S1	–	?	–	–	?	Plugged by moraine GW2
S2	–	?	–	–	?	Plugged by moraine GW2
S3	–	–	–	–	–	Plugged by moraine GW2
S4	–	–	–	–	–	Plugged by moraine GW2
S5	–	? or	?	?	–	Plugged by moraine GW2
S6	–	?	?	–	?	Plugged by moraine GW1
S7	–	?	?	–	?	Plugged by moraine GW1
S8	–	?	?	–	?	Major spillway from western margin

Spillway numbers refer to locations shown in Fig. 2.

Table 4
Synthesis and correlation of glacier fluctuations on the northern slope of Eyjafjallajökull

Cal yr BP	Maximum bounding tephra	Gígjökull moraines	Gígjökull spillways	Steinsholtsjökull moraines	Period
0	H1947				
	K1918	E1 = W1		SW1	
		W2			
		E2	S1 = S2 = S5 to S8	SW2 = SE3	
	E1821	N7	Kettled fans		
					Little
	K1755				
	K1721	N9 = W8		SW3	Ice
				SW4 = SE4	
		W7 = W9	S5 = S6 = S7 = S8	SE5 = SW5	Age
250				SE6	
	H1597				
500					
	H1341				
750		E3	S5		
					Medieval Warm Period
1000					
	V870				
		E4	S1, S2, S6 to S8		Dark Ages
1500					
	SILK YN				
		E5			
		E6			
2000					Subatlantic
	SILK UN				

References

Bergthórsson, P., 1969. An estimate of drift ice and temperature in Iceland in 1000 years. Jökull 19, 94–101.
Bradwell, T., 2001. A new lichenometric dating curve for southeast Iceland. Geografiska Annaler 83A, 91–101.
Bradwell, T., 2004. Lichenometric dating in southeast Iceland: size-frequency approach. Geografiska Annaler 86A, 31–41.
Bradwell, T., Dugmore, A.J., Sugden, D.E., 2006. The Little Ice Age glacier maximum in Iceland and the North Atlantic Oscillation: evidence from Lambatungnajökull, southeast Iceland. Boreas 35, 61–80.
Caseldine, C.J., 1985. The extent of some glaciers in northern Iceland during the Little Ice-Age and the nature of recent deglaciation. Geographical Journal 151, 215–227.
Caseldine, C.J., 1991. Lichenometric dating, lichen population studies, and Holocene glacial history in Tröllaskagi, northern Iceland. In: Maizels, J.K., Caseldine, C. (Eds.), Environmental Change in Iceland: Past and Present. Kluwer Academic Publishers, Dordrecht, Netherlands, pp. 219–236.
Caseldine, C.J., Stötter, J., 1993. "Little Ice Age" glaciation of Tröllaskagi peninsula, northern Iceland: climatic implications for reconstructed equilibrium-line altitudes (ELAs). The Holocene 3, 357–366.
Casely, A.F., Dugmore, A.J., 2004. Climate change and "anomalous" glacier fluctuations: the southwest outlets of Mýrdalsjökull, Iceland. Boreas 33, 108–122.
Dugmore, A.J. (1987). Holocene glacier fluctuations around Eyjafjallajökull, south Iceland: a tephrochronological study. Unpublished Ph.D thesis, University of Aberdeen, 214 pp.

https://doi.org/10.1016/j.yqres.2008.07.001 Published online by Cambridge University Press

Dugmore, A.J., 1989. Tephrochronological studies of Holocene glacier fluctuations in south Iceland. In: Oerlemans, J. (Ed.), Glacier Fluctuations and Climatic Change. Kluwer Academic Publishers, Dordrecht, Netherlands, pp. 37–55.

Dugmore, A., Buckland, P., 1991. Tephrochronology and Late Holocene soil erosion in south Iceland. In: Maizels, J.K., Caseldine, C. (Eds.), Environmental Change in Iceland: Past and Present. Kluwer Academic Publishers, Dordrecht, Netherlands, pp. 147–160.

Dugmore, A.J., Larsen, G., Newton, A.J., Sugden, D.E., 1992. Geochemical stability of fine-grained silicic tephra layers in Iceland and Scotland. Journal of Quaternary Science 7, 173–183.

Dugmore, A.J., Shore, J.S., Cook, G.T., Newton, A.J., Edwards, K.J., Larsen, G., 1995. The radiocarbon dating of tephra layers in Britain and Iceland. Radiocarbon 37, 286–295.

Dugmore, A.J., Newton, A.J., Larsen, G., Cook, G.T., 2000. Tephrochronology, environmental change and the Norse settlement of Iceland. Environmental Archaeology 5, 21–34.

Evans, D.J.A., Archer, S., Wilson, D.J.H., 1999. A comparison of the lichenometric and Schmidt hammer dating techniques based on data from the proglacial areas of some Icelandic glaciers. Quaternary Science Reviews 18, 13–41.

Grönvold, K., Óskarsson, N., Johnsen, S.J., Clausen, H.B., Hammer, C.U., Bond, G., Bard, E., 1995. Ash layers from Iceland in the Greenland GRIP ice core correlated with ocean and land sediments. Earth and Planetary Science Letters 135, 149–155.

Guðmundsson, H.J., 1997. A review of the Holocene environmental history of Iceland. Quaternary Science Reviews 16, 81–92.

Kirkbride, M.P., 2002. Icelandic climate and glacier fluctuations through the terminus of the "Little Ice Age". Polar Geography 26, 116–133.

Kirkbride, M.P., Brazier, V., 1998. A critical evaluation of the use of glacier chronologies in climatic reconstruction, with reference to New Zealand. In: Owen, L.A. (Ed.), Mountain Glaciation, Quaternary Proceedings, 6, pp. 55–64.

Kirkbride, M.P., Dugmore, A.J., 2001a. Can the late "Little Ice Age" glacial maximum in Iceland be dated by lichenometry? Climatic Change 48, 151–167.

Kirkbride, M.P., Dugmore, A.J., 2001b. Timing and significance of mid-Holocene glacier advances in northern and central Iceland. Journal of Quaternary Science 16, 145–153.

Kirkbride, M.P., Dugmore, A.J., 2003. Glaciological response to distal tephra fallout from the 1947 eruption of Hekla, Iceland. Journal of Glaciology 49, 420–428.

Kirkbride, M.P., Dugmore, A.J., 2006. Responses of mountain ice caps in central Iceland to Holocene climate change. Quaternary Science Reviews 25, 1692–1707.

Kjartansson, G., 1967. The Steinsholtshlaup, central-south Iceland on 15 January 1967. Jökull 17, 249–262.

Kugelmann, O., 1991. Dating recent glacier advances in the Svarfadardalur-Skidadalur area of northern Iceland by means of a new lichen curve. In: Maizels, J.K., Caseldine, C. (Eds.), Environmental Change in Iceland: Past and Present. Kluwer Academic Publishers, Dordrecht, Netherlands, pp. 203–217.

Lamb, H.H., 1979. Climatic variation and changes in the wind and ocean circulation: the Little Ice Age in the northeast Atlantic. Quaternary Research 11, 1–20.

Larsen, G., 1981. Tephrochronology by microprobe glass analysis. In: Self, S., Sparks, R.S.J. (Eds.), Tephra Studies. Reidel, Dordrecht, Netherlands, pp. 95–102.

Larsen, G., 1982. Tephrochronology of Jökuldalur and the surrounding areas. In: Thórarindóttir, H. (Ed.), Eldur er í Norðri. Sögufélag Reykjaviku, Reykjavik, Iceland, pp. 51–66.

Larsen, G., 1984. Recent volcanic activity of the Veidivotn fissure swarm, southern Iceland: and approach to volcanic risk assessment. Journal of Volcanology and Geothermal Research 22, 33–58.

Larsen, G., 2000. Holocene eruptions within the Katla volcanic system, south Iceland: characteristics and environmental impact. Jökull 49, 1–28.

Larsen, G., Dugmore, A.J., Newton, A.J., 1999. Geochemistry of historical age silicic tephras in Iceland. The Holocene 9 (4), 463–471.

Larsen, G., Newton, A.J., Dugmore, A.J., Vilmundardóttir, E., 2001. Geochemistry, dispersal, volumes and chronology of Holocene silicic tephra layers from the Katla volcanic system. Journal of Quaternary Science 16, 119–132.

Luterbacher, J., Schmutz, C., Gyalistras, D., Xoplaki, E., Wanner, H., 1999. Reconstruction of monthly NAO and EU indices back to AD 1675. Geophysical Research Letters 26, 2745–2748.

McKinzey, K.M., Orwin, J.F., Bradwell, T., 2004. Re-dating the moraines at Skálafellsjökull and Heinabergsjökull using different lichenometric methods: implications for the timing of the Icelandic Little Ice Age maximum. Geografiska Annaler 86A, 319–335.

Maizels, J.K., Dugmore, A.J., 1985. Lichenometric dating and tephrochronology of sandur deposits, Sólheimajökull area, southern Iceland. Jökull 35, 69–77.

O'Brien, S.R., Mayewski, P.A., Meeker, L.D., Meese, D.A., Twickler, M.S., Whitlow, S.I., 1995. Complexity of Holocene climate as reconstructed from a Greenland ice core. Science 270, 1962–1964.

Ogilvie, A.E.J., 1984. The past climate and sea-ice record from Iceland, part 1: data to A. D.1780. Climatic Change 6, 131–152.

Ogilvie, A.E.J., 1992. Documentary evidence for changes in the climate of Iceland, A.D. 1500 to 1800. In: Bradley, R.S., Jones, P.D. (Eds.), Climate Since A.D. 1500. Routledge, London, pp. 92–117.

Stötter, J., Wastl, M., Caseldine, C., Haberle, T., 1999. Holocene palaeoclimatic reconstruction in northern Iceland: approaches and results. Quaternary Science Reviews 18, 457–474.

Thórarinsson, S., 1944. Tefrokronologiska studier pa Island. Geografiska Annaler 26, 1–217.

Thórarinsson, S., 1967. he eruptions of Hekla in historical times. The eruption of Hekla 1947–1948. Visindafélag Islendinga, Reykjavik, Iceland, pp. 1–170.

Thórarinsson, S., 1980. Langleiðir gjósku úr þremur Kötlugosum. Jökull 30, 65–73.

https://doi.org/10.1016/j.yqres.2008.07.001 Published online by Cambridge University Press